Photoemission study of Pb on Ge(111)

J. A. Carlisle, T. Miller, and T.-C. Chiang
Department of Physics, University of Illinois at Urbana-Champaign, 1110 West Green Street, Urbana, Illinois 61801
and Materials Research Laboratory, University of Illinois at Urbana-Champaign, 104 South Goodwin Avenue, Urbana, Illinois 61801
(Received 10 August 1992)

Photoemission spectroscopy with synchrotron radiation, Auger electron spectroscopy, and high-energy electron diffraction have been used to study the Pb-induced reconstructions of the Pb/Ge(111) system. The Ge 3*d* and Pb 5*d* core levels and valence bands are analyzed as a function of Pb coverage and annealing temperature. We have observed three $(\sqrt{3}\times\sqrt{3})R30°$ reconstructions with ideal Pb coverages of $\frac{1}{6}$, $\frac{1}{3}$, and $\frac{4}{3}$ monolayer (in substrate units), the latter being the completion coverage for the first two-dimensional adlayer following the Stranski-Krastanov growth mode. The band bending for this system will be discussed in the monolayer regime. Surface core levels and surface states were observed which suggest a simple T_4 adatom geometry for the lower coverage $(\sqrt{3}\times\sqrt{3})R30°$ reconstructions.

I. INTRODUCTION

Lead deposits on Si and Ge surfaces have received a large amount of attention recently. Pb monolayers on these substrates have been considered "prototypical" systems with regard to metal-semiconductor interface formation.[1] This is due to the mutual insolubility and nonreactivity of Pb with these substrates, which results in an atomically abrupt interface. These properties eliminate complications in reactive systems where intermixing yields a system which is difficult at best to characterize on an atomic level. This lack of intermixing and reaction coupled with the fact that the Pb melting point is much less than that of Si or Ge also allows the study of two-dimensional (2D) melting of the Pb overlayer.

A fairly large body of work has been published for the Pb/Ge(111) system, yet the phase diagram for this system remains the subject of some debate. Early studies by Métois and Le Lay,[2,3] using low-energy electron diffraction (LEED), Auger electron spectroscopy, and scanning electron microscopy, and by Ichikawa using reflection high-energy electron diffraction (HEED),[4,5] found that Pb grows on Ge(111) in the Stranski-Kastanov (SK or 2D adlayer plus 3D islands) mode. Métois and Le Lay found two $(\sqrt{3}\times\sqrt{3})R30°$ reconstructions, with completion coverages of $\frac{1}{3}$ and 1 monolayer (ML) (in substrate units), labeled the α and β phases, respectively. Ichikawa found completion coverages of $\frac{2}{3}$ and $\frac{4}{3}$ ML for these phases. More recent surface x-ray diffraction work,[6,7] x-ray standing wave,[8] and a dynamical LEED *I-V* analysis,[9] have found a completion coverage of $\frac{4}{3}$ ML for the β phase. Structural models which have been proposed by the various groups are summarized in Fig. 1. The general consensus is that the α phase is composed of $\frac{1}{3}$-ML Pb atoms occupying the so-called T_4 sites (see Fig. 1). The 1.3-ML β phase consists of a 1% compressed, close-packed Pb(111) layer rotated 30° with respect to the Ge substrate, with $\mathrm{Pb}\langle 11\bar{2}\rangle \| \mathrm{Ge}\langle \bar{1}10\rangle$. In this phase, $\frac{1}{3}$-ML Pb atoms are in H_3 sites and the remaining 1-ML Pb atoms are in bridge sites (i.e., between T_1 and T_4 sites). The 1-ML β phase structural models either consist of Pb adatoms in T_4 sites with the Pb(111) adlayer in parallel epitaxy[1,2,10] (see Fig. 1) or a modified honeycomb structure (not shown).[11] In addition to these room-temperature-stable reconstructions, the β phase is known to undergo a reversible phase transition to a (1×1) structure at $T\sim200$ °C; the nature of this phase transition has been the subject of some debate.[2–5,12–14]

In the present work we present a detailed photoemission, Auger, and HEED study of the electronic and atomic structure of the Pb/Ge(111) system. Although some angle-resolved valence-band studies have been made on this system,[10,12,13] to our knowledge no Ge or Pb core-level results have been reported. The Ge 3*d* and Pb 5*d* core levels and valence-band spectra will be analyzed as a function of Pb coverage and annealing temperature. Our measurements confirm the SK growth mode with the 2D adlayer completed at $\sim\frac{4}{3}$ ML. The band bending for this system will be discussed in the monolayer regime. Based on our HEED studies we have found a $(\sqrt{3}\times\sqrt{3})R30°$ reconstruction, in addition to the α and β phases, with an ideal Pb coverage of $\frac{1}{6}$ ML. This phase, which is probably similar in structure to the "mosaic" phase found in recent STM work for the Pb/Si(111) system,[15] will be labeled the γ phase. The Ge 3*d* surface-shifted core levels and surface states near the Fermi level detected for the γ and α phases suggest a simple T_4 adatom geometry. In contrast to our recent work on the Pb/Si(111) system,[16] we have found the γ and α reconstructed surfaces to be strongly metallic: these surfaces have a clearly detectable Fermi edge in the valence-band spectrum.

II. EXPERIMENTAL DETAILS

The photoemission experiments were performed on the 1-GeV storage ring Aladdin at the Synchrotron Radiation Center of the University of Wisconsin—Madison. A large hemispherical analyzer was employed to detect electrons emitted from the sample in an angle-integrating mode. All binding energies were measured relative to the

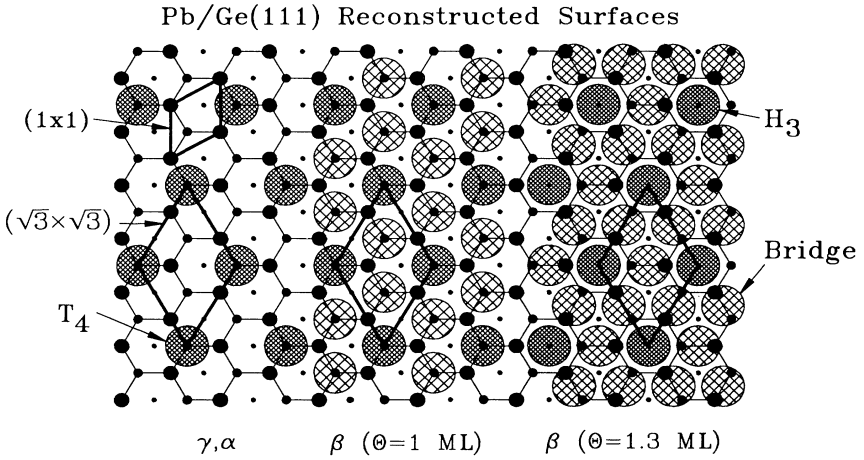

FIG. 1. This figure displays in projection the various structural models proposed for the Pb/Ge(111) system. The α phase is a $(\sqrt{3}\times\sqrt{3})R30°$ reconstruction which consists of $\frac{1}{3}$ ML Pb atoms in T_4 sites. T_4 sites are threefold-symmetric sites located directly above an atom in the second layer. The γ phase (not shown) is also a $(\sqrt{3}\times\sqrt{3})R30°$ reconstruction but with an equal mix of Pb and Ge adatoms in a T_4 registry. Structural models for the higher coverage β phase consist of a close-packed Pb layer in either parallel epitaxy with the Pb adatoms in T_4 sites and a completion coverage of 1 ML (middle) or a 30° rotated close-packed Pb adlayer (right) with a completion coverage of $\frac{4}{3}$ ML. The latter reconstruction consists of Pb adatoms in H_3 sites (threefold sites above fourth-layer Ge atoms) and in bridge sites. The modified honeycomb model (not shown) for the β phase consists of $\frac{1}{3}$-ML Ge adatoms in H_3 sites in 1-ML Pb atoms in bridge sites. The (1×1) and $(\sqrt{3}\times\sqrt{3})R30°$ unit cells are shown.

Fermi level, which was taken from a gold foil in electrical contact with the sample. The overall experimental resolution was between 100–170 meV, depending on the photon energy used. All spectra were acquired with the sample at or near room temperature (RT).

The Ge(111) sample used was oriented with the Laue technique and polished to a mirror finish. The sample was then etched in a CP-4 solution just prior to chamber insertion. Cleaning of the Ge(111) surfaces was performed by several cycles of 0.5-keV Ar-ion bombardment while annealing at 500 °C followed by 15-min anneals at 800 °C. This procedure consistently yields very sharp $c(2\times8)$ HEED patterns as well as strongly pronounced surface-shifted core-level components and well-defined surface-state features in the valence band. High-purity (99.999%) Pb was evaporated from a tungsten crucible heated with a feedback-controlled electron beam. The deposition rate was measured using a quartz-crystal thickness monitor; the uncertainty in absolute coverage was less than $\pm10\%$.[17] The coverage units used throughout this work are referred to the Ge(111) unreconstructed substrate: 1 ML$=7.21\times10^{14}$ atoms/cm^2 =one-half of a Ge(111) double layer.

The core-level decomposition procedure used a nonlinear least-squares method utilizing Voigt line shapes (convolution of a Gaussian and a Lorentzian) to represent each spin-orbit-split component. Each spectrum was assumed to consist of several such doublets, representing the bulk and surface contributions, on top of a cubic polynomial to approximate the secondary-electron background.

III. RESULTS AND DISCUSSION

Our HEED results can be summarized as follows. As Pb is gradually added to the Ge(111)-$c(2\times8)$ surface at RT, the $\frac{1}{2}$-, $\frac{1}{4}$-, and $\frac{1}{8}$-order diffraction spots gradually fade, leaving the characteristic $\frac{1}{3}$-order spots of a $(\sqrt{3}\times\sqrt{3})R30°$ reconstruction. However, the coverage at which this $c(2\times8)$ to $(\sqrt{3}\times\sqrt{3})R30°$ transition is completed was found to occur at $\frac{1}{6}$ ML, not at $\frac{1}{3}$ ML as has been previously observed.[2] This result is not altogether surprising, as similar $\frac{1}{6}$-ML "mosaic" reconstructions have been recently found in the Pb/Si(111) system by STM and isothermal desorption.[15,16] We will label this new submonolayer phase as the γ phase. As more Pb is deposited, the HEED pattern generally improves in quality (as accessed by the sharpness of the diffraction spots, the level of background, and the sharpness of the Kikuchi lines) to $\frac{1}{3}$-ML Pb coverage. In the $\frac{1}{3}$–$\frac{4}{3}$-ML range, the pattern at first becomes worse but then improves again, so that by $\frac{4}{3}$-ML coverage, the general quality of the diffraction pattern is superior as compared to the low-coverage phases. Beyond about 1.5 ML, 3D diffraction spots are observed along the shadow edge, indicative of the formation of 3D Pb islands on the surface.

It is interesting to note that the long-range order noted above based on HEED is opposite to that observed for the Pb/Si(111) system.[16] For the Pb/Si(111) system, the submonolayer phases (denoted γ and β) exhibit greater long-range order than the Pb/Si(111)-α phase (the $\frac{4}{3}$-ML completion phase for this system).[18] We will return to this point later.

The general quality of the diffraction patterns was improved by either depositing Pb on the Ge(111) substrate at elevated temperatures (100–250 °C) or by post RT-deposition annealing to the same temperatures. The surface core levels and surface states found for these reconstructions (to be discussed below) were also improved (sharpened) slightly by the annealing. Since all the basic features of the phase diagram for this system are

unaffected by deposition at these elevated temperatures (which are much less than the Pb melting point of 340 °C), we deposited Pb on Ge(111) substrates maintained at $T=200$ °C, and all of the data presented in this work were obtained using these deposition parameters.

We have studied in detail the modification of the Ge 3*d* and Pb 5*d* core levels and Auger features as a function of Pb coverage. In Fig. 2 we show the evolution of the *I*(Pb *MNN*)/*I*(Ge *LMM*) Auger intensity ratio (top curve), the absolute Pb 5*d* photoemission intensity (middle curve), and the *I*(Pb 5*d*)/*I*(Ge 3*d*) photoemission intensity ratio (bottom curve), versus Pb coverage in ML. The general shape of these curves is indicative of the SK growth mode, with the break point showing the completion coverage of the first adlayer (i.e., the transition point between layer-by-layer and island growth). As can be readily observed, each of the curves increases in a linear fashion with a clearly defined break at $\sim\frac{4}{3}$ ML. This value for the completion coverage agrees with the structural model for the β phase shown in Fig. 1 with $\Theta=\frac{4}{3}$ ML, as first proposed by Feidenhans'l *et al.*[6]

In the following paragraphs we will discuss the band bending for the Pb/Ge(111) system in the monolayer regime. In Fig. 3 is shown the Ge 3*d* core level obtained for the clean Ge(111)-*c*(2×8) surface (lower spectrum) and for the β phase with $\frac{4}{3}$-ML Pb deposited at 200 °C (upper spectrum). These spectra were obtained using a photon energy of $h\nu=40$ eV, which increases the electron escape depth to 10–15 Å and thus reduces the surface sensitivity. These spectra thus contain a significant contribution from Ge atoms in the bulk and are thus bulk sensitive. Ge core levels obtained using 90-eV photons (discussed below) minimize the escape depth (2–5 Å), and are thus surface sensitive. As can be seen in Fig. 3, the bulk Ge $3d_{5/2}$ energy position moves from its value for the clean surface to lower binding energy by 0.225 eV upon formation of the β phase. By obtaining Ge 3*d* cores for various Pb coverages, one may thus track the band bending as a function of Pb coverage.

The binding energy position of the bulk Ge $3d_{5/2}$ component vs Pb coverage is given in Fig. 4. The Ge $3d_{5/2}$ binding energy moves from its value for the clean surface of 29.435 to 29.210 eV for the β phase. Note that the band bending saturates at the same coverage as the curves in Fig. 2. Given a knowledge of the Fermi level pinning position for the clean Ge(111)-*c*(2×8) surface,

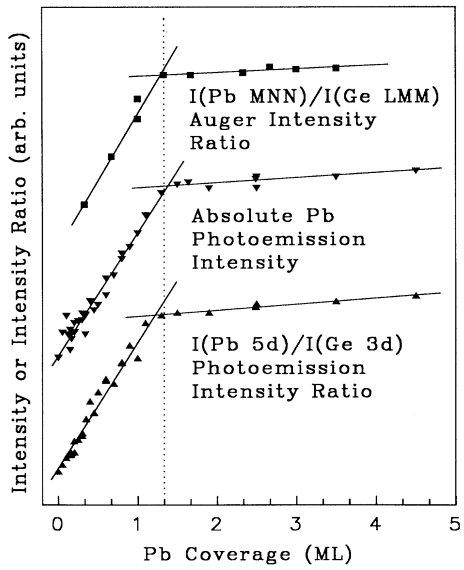

FIG. 2. The Pb/Ge Auger intensity ratio (upper curve), the absolute Pb 5*d* photoemission intensity (middle curve) and the *I*(Pb 5*d*)/*I*(Ge 3*d*) photoemission intensity ratio (bottom curve), are shown vs the number of ML of Pb deposited in substrate units (1 ML$\equiv 7.21\times10^{14}$ atoms/cm^2). The Ge 3*d* intensities were acquired using 40-eV photons (bulk sensitive). The vertical dotted line indicates the completion coverage of the 2D adlayer, $\sim\frac{4}{3}$ ML.

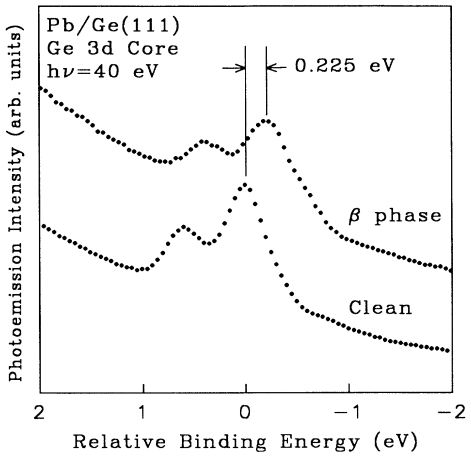

FIG. 3. The Ge 3*d* core level obtained for the clean Ge(111)-*c*(2×8) surface (bottom spectrum), and for the Pb/Ge(111)-β phase (upper curve). Both of these spectra were acquired using 40-eV photons and are thus dominated by contribution from Ge atoms in the bulk. The 0.225-eV shift to lower binding energy shows the band bending induced by the deposition of $\frac{4}{3}$ ML of Pb to form the β phase.

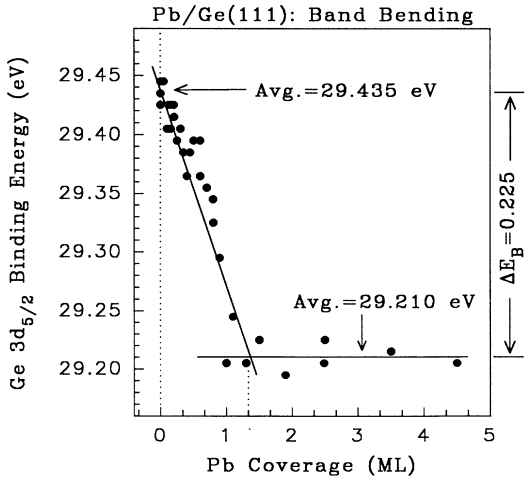

FIG. 4. The Ge $3d_{5/2}$ binding energy (with respect to the Fermi level) is plotted versus the Pb coverage in ML.

one may use these data to track the position of the Fermi level (E_F) with respect to the valence-band maximum (E_{VBM}) versus the Pb coverage. However, in contrast to the Si(111)-(7×7) surface, for which the pinning position is well known (0.65 eV above E_F),[19] the pinning position for the Ge(111)-c(2×8) surface is not firmly established. In the angle-resolved photoemission study of Ref. 10, a value of 0.1 eV is quoted, but this would lead to a final Fermi-level position ~0.1 eV *below the valence-band maximum,* which is unphysical. Based on reported values for the binding energy of the bulk Ge $3d_{5/2}$ component with respect to E_{VBM}, 29.36 (Ref. 20) or 29.10 (Ref. 21), we may utilize our measured value for the binding energy of the Ge $3d_{5/2}$ component, 29.44±0.02, with respect to E_F (determined from a gold foil in electrical contact with the sample), to determine the position of the Fermi level of the clean surface: 0.09 or 0.34 eV above E_{VBM}, respectively. The first value results again in an unphysical final pinning position for the Fermi level, whereas the second yields a value of 0.34−0.225=0.12 eV above the valence-band maximum. We have reason to believe the value of 29.1 eV quoted in Ref. 21 is the more reliable one since this study explicitly took into account the surface state emission near the Fermi level. By using the value of 0.12 eV for the final position of the Fermi level, and by using the band gap of Ge, 0.67 eV, we determine an n-type barrier height of 0.55 eV for the β phase.

We now address the core-level and valence-band line shapes. In Figs. 5–7 we show the Ge 3d core levels, the valence-band spectra, and the Pb 5d cores obtained for the γ, α, and β reconstructed surfaces, and for other Pb coverages of interest. The Ge 3d core-level spectra shown in Fig. 5 were acquired using 90-eV photons, and are thus surface sensitive. The spectrum given at the bottom of Fig. 5 shows the Ge 3d core derived from the clean surface. Its decomposition into three spin-orbit-split components (a bulk component B and two surface components $S1$ and $S2$) has been documented in several previous studies, and are shown in the curves underneath the raw data.[22] The fit is the solid line through the data points. Table I summarizes some of the fitting parameters used.

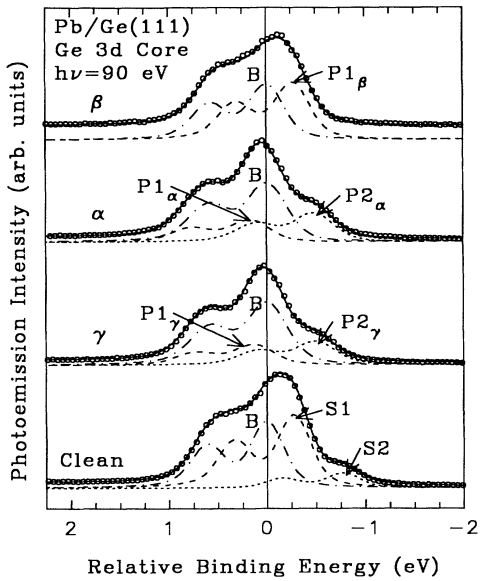

FIG. 5. Ge 3d core-level spectra acquired from clean Ge(111)-c(2×8) and the various Pb/Ge(111) surface phases. The circles are the data points, and the lines through them are the least-squares fits. The surface-shifted components ($S1$ and $S2$ for the clean surface and $P1$ and $P2$ for the Pb covered surfaces) and bulk components (B) are shown as the curves under each spectrum. The relative binding energy scale is referred to the bulk component in each spectrum. See Table I for a list of the fitting parameters.

Based on the qualitative changes of the raw data (circles in Fig. 5), there are significant changes in the surface environment for the Ge atoms. Between 0 and $\frac{1}{6}$ ML, there are drastic changes in the shape of the Ge 3d core-level spectrum. This is not surprising, since the surface reconstruction in this coverage range is changing from a c(2×8) to a $(\sqrt{3}\times\sqrt{3})R30°$ one. For the coverage range $\frac{1}{6}$ to $\frac{1}{3}$ ML (transition from the γ phase to the α phase), the line-shape change is more subtle: increasing intensity on the lower binding energy side of the spectrum. From $\frac{1}{3}$ to $\frac{4}{3}$ ML (from α to β), the line-shape changes are again more pronounced.

Based on the appearance of the raw data acquired for the α phase, there are at least two components which comprise the spectrum. However, attempts to fit this spectrum with only two doublet components led to Gaussian widths much larger than the width which would be expected based on the bulk sensitive spectra. A three-component fit yielded very nice results, as shown in Fig. 5. These three components are labeled B, $P1_\alpha$, and $P2_\alpha$. Based on a comparison of this spectrum with one acquired using 40-eV photons (bulk sensitive, not shown), we deduce that $P1_\alpha$ and $P2_\alpha$ derive from surface emission, whereas B derives from emission from Ge atoms in the bulk. The same statements hold for the B, $P1_\gamma$, and $P2_\gamma$ components of the Ge 3d spectrum found for the γ phase as well as the B and $P1_\beta$ components for the β phase. Similar decompositions were made for the Pb/Si(111) γ and β surfaces.[16]

Looking at Table I and Fig. 5, note that the γ and α core results are very similar: essentially the same surface

TABLE I. Fitting parameters for the surface sensitive Ge 3d core-level spectra acquired for the clean Ge(111)-c(2×8) surface and the γ, α, and β phases. All energies are in eV. The Gaussian and Lorentzian widths refer to the full width at half maximum. Binding energy shifts are referred to the bulk components B.

	c(2×8)	γ phase	α phase	β phase
Spin-orbit splitting	0.600	0.591	0.596	0.584
Branching ratio	0.620	0.591	0.593	0.595
Gaussian width	0.310	0.380	0.392	0.352
Lorentzian width	0.130	0.130	0.130	0.130
$S1$ ($P1$) shift	0.275	−0.180	−0.180	−0.264
$S2$ ($P2$) shift	0.770	0.483	0.474	
$I[S1\ (P1)]/I(S0\ (P0)]$	1.100	0.430	0.427	1.021
$I[S2\ (P2)]/I[S0\ (P0)]$	0.225	0.385	0.520	

shifts and the same $I(P1_{\gamma,\alpha})/I(B)$ intensity ratio. The main difference is the $I(P2_{\gamma,\alpha})/I(B)$ ratio. It changes from 0.385 to 0.520. These data suggest that the $P2$ components are derived from a direct Ge-Pb interaction (i.e., bonding) since the Pb coverage and the $I(P2)/I(B)$ ratio is strongly correlated (i.e., the increase in height of the lower binding energy shoulder with Pb coverage). The $I(P1)/I(B)$ ratios are approximately uncorrelated, so it seems likely that the $P1$ components are subsurface in origin. Comparing the $I(S2)/I(S1+B)$ ratio for the clean Ge(111)-$c(2\times8)$ surface with $I(P2_\alpha)/I(P1_\alpha+B_\alpha)$, and by utilizing the fact that $S2$ represents emission from $\frac{1}{4}$-ML adatoms on the surface,[22,23] we find that the $P2$ component for the α phase represents emission from $\sim$1-ML Ge atoms. In light of the $(\sqrt{3}\times\sqrt{3})R30°$ surface reconstruction, it is likely that the $P2_\alpha$ component represents emission from Ge atoms located in the first half of the first double layer on the Ge substrate bonded to a Pb adatom in either a T_4 or H_3 geometry. The T_4 registry is preferred based on energy minimization calculations,[24] and is shown in Fig. 1.

The T_4 Pb adatom geometry is further supported upon consideration of the valence-band data acquired for the α phase. In Fig. 6 we show several valence-band spectra obtained for the surface phases considered. For the γ and α phases, we have found two well-defined surface states at about 0.3 and 1.2 eV below the Fermi level, as are indicated by the arrows in Fig. 6. Similar surface states were observed for the Pb/Si(111) system,[16] and have also been reported for the Al/Si(111)-$(\sqrt{3}\times\sqrt{3})R30°$ surface.[25] The atomic origin of these surface states is known to be due to the adatom complex: the lower binding energy surface state (0.3 eV) is principally derived from adatom dangling p_z orbitals, whereas the higher binding energy state (1.2 eV) is derived from

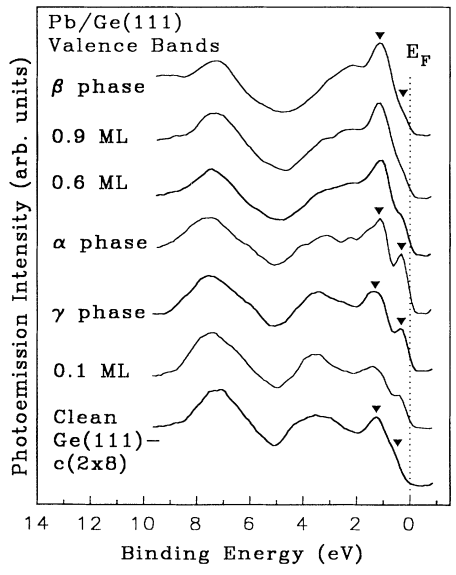

FIG. 6. Valence-band spectra acquired for the clean Ge(111)-$c(2\times8)$ surface, the γ, α, and β phases, and other Pb coverages of interest. The triangles indicate surface-state positions.

adatom p_{xy} orbitals (oriented in the plane of the surface) coupled to substrate Ge dangling p_z orbitals of the bulk-truncated Ge(111) substrate.[23] These valence-band data thus further corroborate our analysis of the Ge $3d$ core for the α phase.

The valence-band spectra acquired for the α and γ phases are very similar. The main difference is that the surface states appear somewhat broader for the γ phase as compared to the α phase. The fact that the "same" surface states are detected for these phases is not surprising, given consideration of recent work on the Pb/Si(111) system. Ganz *et al.*[15] found with STM that the γ (mosaic) phase consists of an equal density of Pb and Si adatoms, randomly distributed in T_4 sites. It is likely, because of the similarity between Pb/Si and Pb/Ge systems, that the Pb/Ge-γ phase is also a mosaic phase. In other words, the $\frac{1}{6}$-ML γ phase of the Pb/Ge system is related to the $\frac{1}{3}$-ML α phase by replacing one-half of the Pb adatoms in the T_4 sites by Ge adatoms. Since all of the T_4 sites on the surface are still occupied by either a Pb or a Ge adatom, the same surface states should exist with the same intensity on both surfaces. The differing atomic species of the adatoms on the surface may alter the energy and/or dispersion of these surface states, which may in turn result in their broadened appearance when viewed in our angle-integrated geometry. Our photoemission data for the Pb/Si(111) system has shown a similar finding.

A surprising difference between the Pb/Si(111) and Pb/Ge(111) systems is that the Pb/Ge(111)-γ,α surfaces are *metallic*, as opposed to the Pb/Si(111)-γ,β surfaces, which are at best weakly metallic.[16] The valence-band spectra shown in Fig. 6, acquired from the γ and α surfaces, both show significant emission at the Fermi level, whereas the valence band acquired from the Pb/Si(111) surfaces show little intensity at the Fermi level. Actually, based on simple electron counting, one would expect these $(\sqrt{3}\times\sqrt{3})R30°$ surfaces with group-IV adatoms in T_4 registries to be metallic, since the adatom dangling bond surface band should be partially filled.[24] As was pointed out in a recent angled-resolved photoemission study,[26] this could indicate that the surface structure for the Pb/Si(111)-$(\sqrt{3}\times\sqrt{3})R30°$ phases is more complicated than a simple T_4 adatom geometry.

The main difference between the Ge $3d$ cores observed for the γ and α phases (see Fig. 5) is a decrease in intensity on the lower binding energy side of the spectrum (the $P2$ component). Based on the fit, the decrease in intensity is about 25%. Since the $P2_\alpha$ component for the α phase corresponds to the top monolayer of Ge atoms in direct bonding to Pb, we would expect this component to be reduced in intensity by 50% upon replacing half the Pb adatoms on the surface with Ge adatoms in going from the α phase to the γ phase. Ge atoms in the first monolayer bonded to Ge adatoms should not display the same shift in binding energy compared to those which make up the $P2_\alpha$ component. One might, however, expect the $\frac{1}{6}$-ML Ge adatoms for the γ phase to display a core-level shift of about -0.77 eV relative to the bulk, in comparison to the $S2$ (adatom) component for the clean Ge(111)-$c(2\times8)$ surface.[22] If we ignore the small energy

difference between the $S2$ and $P2_{\gamma,\alpha}$ shifts, we would expect an intensity reduction of the $P2$ peak from 1 ML for the α phase to $\frac{1}{2}+\frac{1}{6}=\frac{2}{3}$ ML for the γ phase. This predicted intensity decrease of 33% is close to the experimentally observed reduction of 25% mentioned above.

As the Pb coverage increases from $\frac{1}{3}$ to $\frac{4}{3}$ ML, more pronounced changes are observed in the Ge $3d$ core-level and valence-band spectrum (shown in Figs. 5 and 6). The Ge core-level spectrum acquired for the β phase can be fit quite nicely with two components (see Table I). The intensity of the $P1_\beta$ component is consistent with its assignment to emission from a full double layer of Ge atoms. Once again, it is interesting to compare the results here with our recent study of the Pb/Si(111) system. The Pb/Si(111)-α phase, which has about the same completion coverage as the Pb/Ge-β phase, also consists of a close-packed Pb layer rotated 30° with respect to a (bulk-truncated) Si(111) substrate. In contrast to the Pb/Ge(111)-β phase, this reconstruction is slightly incommensurate [i.e., not a perfect $(\sqrt{3}\times\sqrt{3})R30°$ reconstruction]. Despite the similarity of these two reconstructions, the Si $2p$ and Ge $3d$ cores are quite different. Whereas the Ge $3d$ core displays two components (B and $P1_\beta$), the Si $2p$ core essentially consists of only one doublet component.[16] This means that the Pb overlayer, in the case of Ge, does not provide a bulklike environment for the Ge atoms located in the first double layer underneath the Pb. How this difference relates to the reconstruction difference (commensurate vs incommensurate) and lattice mismatch is a matter of speculation.

As the Pb coverage exceeds $\frac{1}{3}$ ML, the surface states associated with the adatom complex become more diffuse (see Fig. 6). Although more difficult to see in our angle-integrated geometry, we still can discern the two surface states in the valence band for the β phase, as reported by Tonner *et al.*[10] (see triangles in Fig. 6). In this study these surface states were attributed to Pb adatoms in a T_4 registry, but the 1-ML reconstruction consistent with this assignment is inconsistent with the completion coverage of $\frac{4}{3}$ ML discussed previously. Based on the structural model in Fig. 1 and our photoemission data, we feel that the lower binding energy surface state at -0.3 eV below the Fermi level is most probably due to Pb dangling p_z bonds from the Pb atoms in an H_3 geometry, whereas the higher binding energy state at -1 eV arises from Pb p_{xy} orbitals.

The Pb $5d$ core levels, obtained for the various reconstructed surfaces considered, are shown in Fig. 7. The most notable aspect of the Pb core-level data is the dependence of the Pb $5d_{5/2}$ full width at half maximum (FWHM) on the Pb coverage. This dependence is illustrated in Fig. 8. The varying width of the Pb $5d$ core is likely a result of multiple unresolved components in the system due to the presence of inequivalent sites and/or due to the varying degrees of long-range ordering of these surfaces. Initially, for very small coverages ($<\frac{1}{6}$ ML), the FWHM is -0.72 eV. As the γ phase is completed, the FWHM decreases to a minimum of -0.62, but as the coverage approaches $\frac{1}{3}$ ML it increases to almost 0.75 eV [see Fig. 8(b)]. This behavior of the Pb FWHM is surprising, since the HEED pattern and surface states both are "sharper" for the α phase as compared to the γ phase. The structural model for the γ phase involves

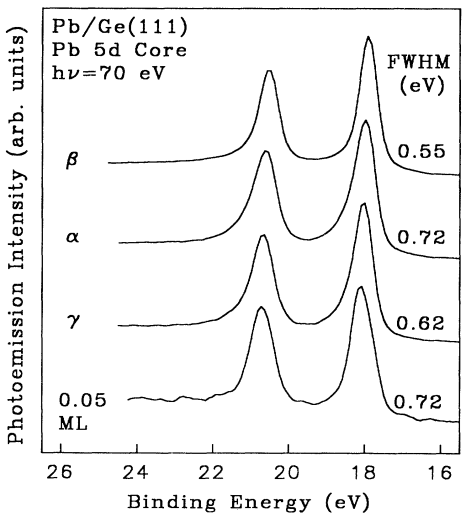

FIG. 7. Pd $5d$ core levels acquired for the γ, α, and β surface phases and a 0.05-ML deposit. The photon energy used was 70 eV. The full width at half maximum (FWHM) of the Pb $5d_{5/2}$ component is recorded to the right of each spectrum.

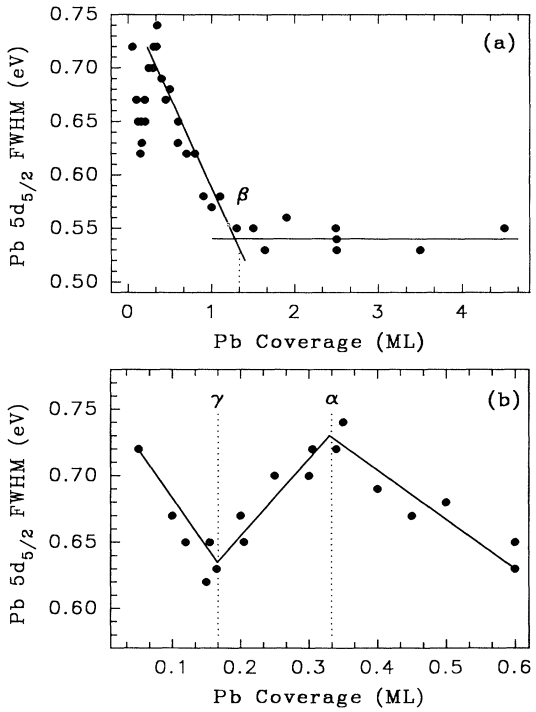

FIG. 8. Dependence of the Pb FWHM vs the Pb coverage in ML. The upper panel (a) shows this dependence for the entire Pb coverage range considered, whereas the lower panel (b) shows the dependence in more detail for the 0.0–0.6-ML range. The lines shown are a guide to the eye. Note that the Pb FWHM saturates at the same coverage as the curves in Fig. 2.

random replacement of one half of the Pb adatoms by Ge adatoms; this randomness could induce broadening. A similar dependence of the Pb FWHM was found in the Pb/Si(111) system.[16] At the present time, we do not have a good explanation for this behavior. As the Pb coverage increases beyond $\frac{1}{3}$ ML, the Pb FWHM decreases rapidly from 0.75 to 0.54 eV at the completion of the 2D adlayer, the narrowest value observed for the Pb/Ge system. The dependence of the FWHM on Pb coverage in this coverage range is reversed as compared to the dependence displayed by the Pb/Si(111) system.

IV. SUMMARY

Photoemission spectroscopy utilizing synchrotron radiation, Auger electron spectroscopy, and high-energy electron diffraction have been used to study the electronic and geometrical structure of the Pb-induced reconstructions of the Pb/Ge(111) system. Our photoemission and Auger measurements have confirmed the SK growth mode for this system, and have found a completion coverage of $\frac{4}{3}$ ML for the β phase. A structural model first proposed by Feidenhans'l *et al.*,[6] which consists of Pb atoms in H_3 and bridge sites, and which is consistent with this completion coverage, is thus corroborated. The band bending induced by the Pb overlayer has been studied in the monolayer regime, whereupon we determined an n-type Schottky barrier height of 0.55 eV. Based on our HEED study and the measured FWHM of the Pb 5d core, we have found a new $\frac{1}{6}$-ML $(\sqrt{3}\times\sqrt{3})R30°$ reconstruction. This is the γ phase. Our detailed core-level and valence-band photoemission data are consistent with a simple adatom geometry for the submonolayer γ and α phases. The α phase consists of $\frac{1}{3}$-ML Pb adatoms in a T_4 geometry, whereas the γ phase consists of $\frac{1}{6}$-ML Pb adatoms and $\frac{1}{6}$-ML Ge adatoms. The varying degrees of ordering of these surfaces have been addressed. Interesting comparisons have been made between the Pb/Ge(111) and Pb/Si(111) systems; the differences might be related to effects of lattice mismatch on the surface morphology and electronic structure.

ACKNOWLEDGMENTS

This work was supported by the U.S. Department of Energy (Division of Materials Sciences, Office of Basic Energy Sciences), under Grant No. DEFG02-91ER45439. Acknowledgment is also made to the Donors of the Petroleum Research Fund, and to the U.S. National Science Foundation (Grant No. DMR-89-19056) for partial support of the beam line. We acknowledge the use of the central facilities of the Materials Research Laboratory of the University of Illinois, which is partially supported by the U.S. Department of Energy and the U.S. National Science Foundation. The Synchrotron Radiation Center of the University of Wisconsin—Madison is supported by the U.S. National Science Foundation.

[1]G. Le Lay, K. Hricovini, and J. E. Bonnet, Appl. Surf. Sci. **41/42**, 25 (1989).
[2]J. J. Métois and G. Le Lay, Surf. Sci. **133**, 422 (1983).
[3]G. Le Lay and J. J. Métois, Appl. Surf. Sci. **17**, 131 (1983).
[4]T. Ichikawa, Solid State Commun. **46**, 827 (1983).
[5]T. Ichikawa, Solid State Commun. **49**, 59 (1983).
[6]R. Feidenhans'l, J. S. Pedersen, M. Nielsen, F. Grey, and R. L. Johnson, Surf. Sci. **178**, 927 (1986).
[7]R. Fiedenhans'l, F. Grey, N. Nielsen, and R. L. Johnson, *Kinetic Ordering and Growth at Surfaces* (Plenum, New York, 1990), p. 189.
[8]B. N. Dev, F. Grey, R. L. Johnson, and G. Materlik, Europhys. Lett. **6**, 311 (1988).
[9]H. Huang, C. M. Wei, H. Li, B. P. Tonner, and S. Y. Tong, Phys. Rev. Lett. **62**, 559 (1989).
[10]B. P. Tonner, H. Li, J. Robrecht, M. Onellion, and J. L. Erskine, Phys. Rev. B **36**, 989 (1987).
[11]H. Li and B. P. Tonner, Surf. Sci. **193**, 10 (1988).
[12]B. P. Tonner, H. Li, J. Robrecht, Y. C. Chou, M. Onellion, and J. L. Erskine, Phys. Rev. B **34**, 4386 (1986).
[13]G. Le Lay and M. Abraham, *Kinetic Ordering and Growth at Surfaces* (Ref. 7), p. 209.
[14]F. Grey, R. Feidenhans'l, J. S. Pedersen, M. Nielsen, and R. L. Johnson, Phys. Rev. B **41**, 9519 (1990).
[15]E. Ganz, F. Xiong, Ing-Shouh Hwang, and J. Golovchenko, Phys. Rev. B **43**, 7316 (1991).
[16]J. A. Carlisle, T. Miller, and T.-C. Chiang, Phys. Rev. B **45**, 3400 (1992).
[17]D. H. Rich, T. Miller, and T.-C. Chiang, Phys. Rev. Lett. **60**, 357 (1988).
[18]Although the phase diagrams for the stable phases of the Pb/Si(111) and Pb/Ge(111) systems are essentially identical (same completion coverages), the denotation of the phases is different. For the Pb/Si(111) system, the reconstructions are labeled γ, β, and α for increasing Pb coverages. For the Pb/Ge(111) system, the phases are labeled γ, α, and β for increasing Pb coverages.
[19]F. J. Himpsel, F. R. McFeely, J. F. Morar, A. Taleb-Ibrahimi, and J. A. Yarmoff, in *Photoemission and Adsorption Spectroscopy of Solids and Interfaces with Synchrotron Radiation,* Proceedings of the International School of Physics "Enrico Fermi," Course CVIII, edited by G. Scoles (North-Holland, New York, 1991).
[20]E. A. Kraut, R. W. Grant, J. R. Waldrop, and S. P. Kowalczyk, Phys. Rev. B **28**, 1965 (1983).
[21]D. E. Eastman and J. L. Freeouf, Phys. Rev. Lett. **33**, 1601 (1974).
[22]See, for instance, T. Miller, T. C. Hsieh, P. John, A. P. Shapiro, A. L. Wachs, and T.-C. Chiang, Phys. Rev. B **33**, 4421 (1986).
[23]T.-C. Chiang, CRC Crit. Rev. Solid State Mater. Sci. **14**, 269 (1988).
[24]John E. Northup, Phys. Rev. Lett. **57**, 154 (1986).
[25]R. I. G. Ubrberg, G. V. Hansson, J. M. Nicholls, and P. E. S. Persson, Phys. Rev. B **31**, 3805 (1985).
[26]C. J. Karlsson, E. Landemark, Y.-C. Chao, and R. I. G. Uhrberg, Phys. Rev. B **45**, 6321 (1992).